Absorption dispersion below boson peak frequency in oxide glasses studied by THz-time domain spectroscopy

Wada, Osamu
Ramachari, Doddoji
Yang, Chan-Shan
Uchino, Takashi
Pan, Ci-Ling

(Citation)
Journal of Applied Physics,135(8):085108

(Issue Date)
2024-02-28

(Resource Type)
journal article

(Version)
Version of Record

(URL)
https://hdl.handle.net/20.500.14094/0100489458

Journal of Applied Physics

RESEARCH ARTICLE | FEBRUARY 27 2024

Absorption dispersion below boson peak frequency in oxide glasses studied by THz-time domain spectroscopy

Osamu Wada ; Doddoji Ramachari ; Chan-Shan Yang ; Takashi Uchino ; Ci-Ling Pan

J. Appl. Phys. 135, 085108 (2024)
https://doi.org/10.1063/5.0191384

AIP Publishing

Journal of Applied Physics ARTICLE pubs.aip.org/aip/jap

Absorption dispersion below boson peak frequency in oxide glasses studied by THz-time domain spectroscopy

Cite as: J. Appl. Phys. **135**, 085108 (2024); doi: 10.1063/5.0191384
Submitted: 13 December 2023 · Accepted: 4 February 2024 ·
Published Online: 27 February 2024

Osamu Wada,[1,2,a)] Doddoji Ramachari,[3,4] Chan-Shan Yang,[5,6] Takashi Uchino,[7] and Ci-Ling Pan[1]

AFFILIATIONS

[1]Department of Physics, National Tsing Hua University, Hsinchu 30013, Taiwan
[2]Office for Academic and Industrial Innovation, Kobe University, Kobe 657-8501, Japan
[3]Institute of Research and Development, Duy Tan University, Da Nang 550000, Vietnam
[4]Faculty of Natural Sciences, Duy Tan University, Da Nang 550000, Vietnam
[5]Institute and Undergraduate Program of Electro-Optical Engineering, National Taiwan Normal University, Taipei 11677, Taiwan
[6]Micro/Nano Device Inspection and Research Center, National Taiwan Normal University, Taipei 106, Taiwan
[7]Graduate School of Science, Kobe University, Kobe 657-8501, Japan

[a)]**Author to whom correspondence should be addressed:** fwga3962@nifty.com

ABSTRACT

The dispersion properties of the absorption coefficients [$\alpha(\nu)$] of different multi-component silicate oxide glasses have been studied in the frequency region below the boson peak by using THz-time-domain spectroscopy. The value of $\alpha(\nu)/\nu^2$ has been shown to exhibit a minimum level (R) at low frequency and subsequently a linear increase in the form of $r(\nu/\nu_{BP} + E)$ with increasing frequency, where ν_{BP} is the boson peak frequency and R, r, and E are material-specific constants. It has also been found that $R \propto r$ and E is a constant common to most glasses. This $\alpha(\nu)/\nu^2$ behavior is ascribed to the dispersion property of the light-vibration coupling coefficient under the reasonable vibrational density of state function. The minimum (constant) and linear terms of the $\alpha(\nu)/\nu^2$ spectrum are originated from the physical/chemical disorder-induced charge fluctuations in the long-range scale (constant term) and short-range scale (linear term), respectively. The fluctuating charge (σ_1) caused by uncorrelated, long-range disorders has primary significance for determining the sub-THz absorption dispersion properties, and its value has been determined for each glass material.

I. INTRODUCTION

Recent advancement of terahertz (THz) technology has widened its application covering various fields such as communication, imaging, sensing, and characterization.[1–4] Glass materials are essential for preparing components required for constructing those THz systems. In particular, high-refractive index, low-absorption loss glasses are highly demanded for applying to various devices and component including not only passive components[5,6] such as waveguides, fibers, and lenses but also active or nonlinear components[7,8] such as amplifiers, modulators, switches, and frequency converters. For designing better materials and components, in-depth characterization of dielectric and absorption properties in the THz frequency range is indispensable. THz-time-domain spectroscopy (THz-TDS)[9–11] is highly suitable for such characterization due to its advantage of the capability of independent determination of the refractive index and absorption coefficient with high accuracy and has been applied by many researchers for accessing various oxide and chalcogenide glasses.[12,13]

Naftaly's group has reported THz dielectric properties of various commercial oxide glasses[14] and chalcogenide glasses[15] using THz-TDS measurements. We have developed oxyfluorosilicate (OFS) glasses, which exhibit high-refractive index (2.9–3.7) and low-loss (6–9 cm^{-1}) properties in comparison to other multi-component oxide glasses at sub-THz frequency, and investigated the mechanism of

dielectric constant enhancement in OFS glasses.[16,17] More recently, Pacewicz has performed precise determination of dielectric properties of a variety of oxide glasses in a wider frequency range covering from 0.15 to 200 THz.[18] THz dielectric properties of other groups of glasses, such as borosilicate,[19] aluminosilicate,[20,21] tellurite,[19] and chalcogenide glasses,[19] have recently been investigated by THz-TDS.

Absorption characteristics in the sub-THz and THz ranges are very important not only for practical device applications but also for understanding physics of low-frequency vibrational properties in glasses. Frequency dependence of the absorption coefficient has been analyzed by the power low relationship that has been first proposed by Strom *et al.*,[22,23] in which absorption is regarded to be caused by fluctuation in the charge distribution in the glass structure. On the other hand, it has been widely known that many amorphous materials show vibration mode called boson peak (BP) in the frequency range around 1 THz,[24,25] in which the vibrational density of state [vDOS $g(\nu)$, where ν is the frequency] is in excess of the Debye level [$g(\nu)/\nu^2$]. Boson peak appearance has been interpreted by various models such as fluctuating elastic constants in the disordered structure,[26,27] quasi-localized soft potential defects,[28,29] broadened transverse-acoustic van Hove singularity,[30,31] dispersionless surface phonon band,[32] and several others (refer to Refs. 33 and 34 and references therein). Although the physical origin of boson peak appearance is still elusive, there have been many reports on significant BP signals in (sub-)THz absorption spectra in various glass materials.[18,25,35,36] Thus, to study the absorption dispersion characteristics at low-frequency (sub-THz) range in glasses, it is required to consider not just the acoustic phonon modes but boson peak contributions. In this respect, the absorption dispersion properties have been studied so far in glasses with simple structures such as silica,[35,36] but multi-component glasses have not been characterized extensively, particularly around and below the BP frequencies.

In this work, we investigate on the absorption characteristics of a series of multi-component silicate oxide glasses by using data collected by THz-TDS measurements. We focus on the frequency dependence of the absorption coefficient [$\alpha(\nu)$] and $\alpha(\nu)/\nu^2$ in the sub-THz frequency region particularly below the boson peak. We aim to examine whether or not there can be found any common feature in the frequency-dependent absorption characteristics in the present glass group. The most striking results we have observed is that $\alpha(\nu)/\nu^2$ value is expressed by a common linear function of the normalized frequency (ν/ν_{BP}, where ν_{BP} is the boson peak frequency) for most glasses in the present group. We discuss physical aspects including a possible mechanism of the observed feature of the absorption dispersion characteristics.

II. EXPERIMENTAL PROCEDURE AND DATA COLLECTION

The multi-component silicate oxide glass series adopted in this study consists of OFS glasses (ZNbKLSNd and PbNKLSNd glasses) and other commercial silicate oxide glasses such as Pyrex and BK7 (borosilicate glasses), SK10 (dense barium glass), and FS10 and FS6 (dense flint glasses), the same glass groups as selected in our previous works.[16,17,37–39] Compositions and measured values of basic physical parameters of glasses such as the molecular weight M, specific density ρ, and molar volume $V_m = M/\rho$ are summarized in Table I. OFS glasses samples were grown by the melt-quenching technique and were sliced and polished into ~1.6 mm thick disks as described in our previous paper.[16] The THz dielectric and absorption properties of OFS glasses were measured by using a transmission-type THz-TDS system, in which a Ti-sapphire laser with the pulse width of 60 fs and the wavelength of 800 nm and a pair of low-temperature grown GaAs-based photoconductive antenna devices were used for THz generation and detection.[16,40] The frequency dependences of the real and imaginary parts of dielectric constants were obtained in the frequency range of 0.2–0.95 THz. The method used for parameter evaluation and substantial part of the result of THz-TDS measurements have been reported in Refs. 16 and 17. As for commercial glasses and fused silica glass, the THz spectral data were taken from Naftaly's publications.[12,14] Dielectric properties of OFS glasses in the optical

TABLE I. Compositions and basic physical parameters of a variety of silicate oxide glasses. Source data have been taken from Ramachari *et al.*, J. Appl. Phys. **125**, 151609 (2019). Copyright 2019 AIP Publishing LLC.[16]

Glass	Composition		M (g/mol)	ρ (g/cm^3)	V_m (cm^3/mol)
ZNbKLSNdx	$(20-x)ZnF_2 + 20Nb_2O_5 + 20K_2CO_3 + 10LiF + 30SiO_2 + xNd_2O_3$	$x = 1$	124	3.65	34.0
		$x = 5$	133	3.66	36.3
		$x = 10$	145	3.54	41.0
PbNKLSNdx	$(20-x)PbF_2 + 5Na_2O + 20K_2CO_3 + 10LiF + 45SiO_2 + xNd_2O_3$	$x = 1$	110	3.72	29.7
		$x = 5$	114	3.78	30.2
		$x = 10$	119	3.62	32.8
Silica	SiO_2		60	2.20	27.3
Pyrex	$80.6SiO_2 + 12.6B_2O_3 + 4.2Na_2O + 2.2Al_2O_3 + 0.04Fe_2O_3 + 0.1CaO + 0.05MgO + 0.1Cl$		62	2.23	27.8
BK7	$68.9SiO_2 + 10.1B_2O_3 + 8.8Na_2O + 8.4K_2O + 2.8BaO + 1.0As_2O_3$		65	2.51	26.0
SK10	$30.6SiO_2 + 11.7B_2O_3 + 5.0Al_2O_3 + 0.1Na_2O + 48.2BaO + 2.0ZnO + 0.7PbO + 0.8Sb_2O_3 + 0.9As_2O_3$		112	3.64	30.8
SF10	$35.3SiO_2 + 2.0Na_2O + 2.5K_2O + 55.7PbO + 4.0TiO_2 + 0.5As_2O_3$		153	4.28	35.8
SF6	$27.7SiO_2 + 0.5Na_2O + 1.0K_2O + 70.5PbO + 0.3As_2O_3$		177	5.18	34.2

frequency range have been evaluated by using the conventional Fourier transform infrared (FTIR) spectroscopy system (Bruker VERTEX 70v) for reference.[39]

III. RESULTS AND DISCUSSION

A. Dispersion of absorption coefficient

The refractive index [$n(\nu)$] and absorption coefficient [$\alpha(\nu)$] spectra have been deduced from THz-TDS measurements on all OFS glasses, and the results have been reported already.[16] Figure 1 shows the product $n(\nu)\alpha(\nu)$ plotted as a function of the THz frequency for ZNbKLSNd (x = 10) and PbNKLSNd (x = 05) glasses as well as other multi-component oxide glasses. In the OFS glass data, although weak oscillatory behaviors are observed at higher frequencies possibly due to residual reflection/scattering related effect in the system, this is not too severe to affect the evaluations of basic dielectric parameters. This has been confirmed by the test measurement using another THz-TDS system (Teraview system) that gave similar parameter values. OFS glasses, in particular, ZNbKLSNd glasses, exhibit refractive indices as high as 3.70 at 0.5 THz, being the highest for silicate oxide glasses.[16] Also the absorption coefficients observed in OFS glasses are significantly lower than those of other glasses known as high-refractive index multi-component glasses.[16]

A comprehensive physical model of far infrared absorption in solids was discussed for various amorphous materials by Strom *et al.*,[22,23] in which disorder-induced charge fluctuations in the material structure cause the coupling of THz radiation into atomic vibration modes. In this model, the product of $n(\nu)$ and $\alpha(\nu)$ is

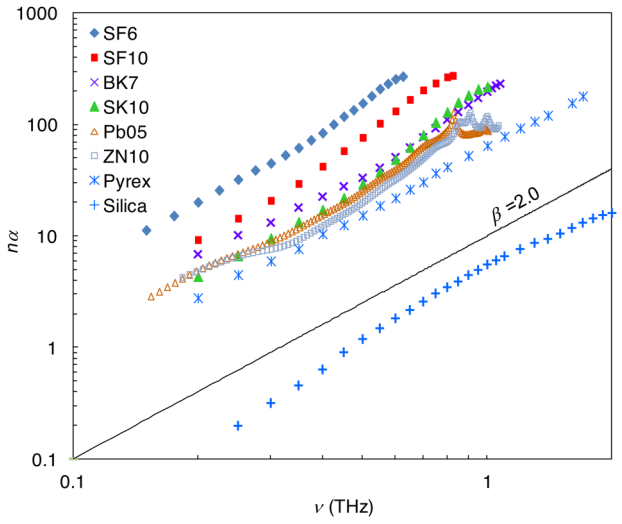

FIG. 1. Absorption coefficient refractive index product plotted as a function of frequency for OFS [ZNbKLSNd (ZN) and PbNKLSNd (Pb)] glasses and other silicate oxide glasses. A straight line indicates the slope for β = 2. Data of other silicate oxide glasses have been taken from M. Naftaly and R. E. Miles, J. Appl. Phys. **102**, 043517 (2007). Copyright 2007 AIP Publishing LLC.

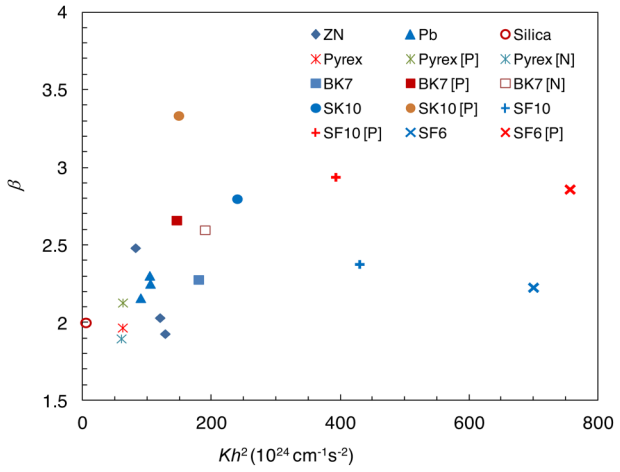

FIG. 2. Values of β parameter plotted as a function of absorption parameter Kh^2 for various silicate oxide glasses as measured by different groups. [P] and [N] indicate Refs. 12 and 18, respectively.

shown to follow a power-law relationship as expressed by[22,23]

$$\eta(\nu)\alpha(\nu) = K(h\nu)^{\beta}, \tag{1}$$

where K and β are material-dependent parameters of each glass and h is Planck's constant. We have analyzed the present OFS glasses on the basis of this relationship. The $n(\nu)\alpha(\nu)$ vs ν behaviors as shown in Fig. 1 are in fairly good agreement with the slope of 2 in the central frequency regions. The absorption parameter K (or Kh^2) can be determined for $\beta = 2$ for these glasses as reported in Ref. 16. This feature is consistent with other results obtained for a number of amorphous materials,[22,23] including silicate[14,18] and chalcogenide[15,19] glasses, which supports the disorder-induced-charge fluctuation model. On the other hand, the exact value of β is basically dependent on the frequency and can be determined from the $n\alpha$ vs ν relationship. In Fig. 2, the values of β as determined by different reports[14,16,18] are plotted vs the Kh^2 value as determined above. As is observed in Fig. 2, no simple, straightforward trend is found, and also the β value varies over a wide range (2–3.4) depending on the materials as well as the measurement frequency (0.5[14,16] and 0.63 THz[18]), implying a necessity of alternative method of characterizing the absorption coefficient dispersion.

B. Dispersion analysis using $\alpha(\nu)/\nu^2$ spectrum and boson peak frequency

Within the linear response theory,[41] the absorption coefficient $\alpha(\nu)$ of disordered material is related to the vibrational density of states (vDOS) $g(\nu)$ by the following equation:[41,42]

$$\alpha(\nu) = C_{abs}(\nu)g(\nu), \tag{2}$$

where $C_{abs}(\nu)$ is the light (THz wave)-vibration coupling coefficient. In the Debye model that assumes a single acoustic branch

with a constant sound velocity, the frequency dispersion of vDOS is known to be represented in a quadratic form $[g(\nu) \propto \nu^2]$.[43] By rewriting Eq. (2), $\alpha(\nu)/\nu^2$ can be expressed by

$$\frac{\alpha(\nu)}{\nu^2} = C_{abs}(\nu)\frac{g(\nu)}{\nu^2}. \tag{3}$$

Boson peak is defined as a peak in the $g(\nu)/\nu^2$ spectrum in excess of the Debye level,[44] and it is reflected in the $\alpha(\nu)/\nu^2$ spectrum. By monitoring the $\alpha(\nu)/\nu^2$ peaks through the THz-TDS measurements, boson peaks have been detected and analyzed in silica glass[35,45] and other amorphous materials.[46–49]

In Fig. 3, the frequency dependence of $\alpha(\nu)/\nu^2$ is shown for various silicate oxide glasses in (a), and results for all OFS glasses are shown in (b) (ZNbKLSNd glasses) and (c) (PbNKLSNd glasses). If the absorption at low frequency obeys the Debye model, $\alpha(\nu)/\nu^2$ would exhibit a constant value, and the boson peak appears as a peak in $\alpha(\nu)/\nu^2$. The boson peak frequencies (ν_{BP}) have been determined from these data, and the results are listed in Table II. In Table II, data in the first three columns (α, Kh^2, and β) except for OFS glasses have been taken from Naftaly's publication.[14] The boson peak frequency determined for silica is 1 THz, being consistent with other reports.[25,26] Below the boson peak frequency, most glasses show gradual decrease of $\alpha(\nu)/\nu^2$ down to the minimum or constant value (defined as R). Further below those frequencies, some glasses show slow increases of $\alpha(\nu)/\nu^2$. Similar $\alpha(\nu)/\nu^2$ increase at lower frequency has been seen in silica[35,50] and other glassy materials.[46,48] The origin of such behavior is not clear but may be related to the extrinsic effects such as the relaxation of impurity- or additive atom-induced dipoles rather than the intrinsic vibrational modes.[51] In this work, we focus on the $\alpha(\nu)/\nu^2$ behavior at the frequency above this region up to the boson peak frequency.

In order to discuss the $\alpha(\nu)/\nu^2$ behavior near the BP, $\alpha(\nu)/\nu^2$ values are plotted as functions of the frequency normalized by the boson peak frequency (ν/ν_{BP}) in Fig. 4. As is visualized unambiguously in the figure, slowly varying parts of the $\alpha(\nu)/\nu^2$ between the minimum (constant level) and the maximum (at ν_{BP}) can be approximated by linear fitting except for SK10 glass. According to our test to find the best fit of the variation of $\alpha(\nu)/\nu^2$ using a form $(\nu - \nu_0)^q$, where ν_0 is the inflection frequency where $\alpha(\nu)/\nu^2$ starts to rise, it has been found that q is in the range from 0.65 to 1.06 for most glasses and is 1.36 for SK10 glass. In the present analysis, we have adopted linear fitting ($q = 1$) for most glasses and quadratic fitting ($q = 2$) for SK10 glass, as shown in Fig. 4. The most striking finding in this result is that the extrapolation of all the straight lines fitted for the varying parts of $\alpha(\nu)/\nu^2$ converge to a common point at $\nu/\nu_{BP} \sim -0.4$. Therefore, the frequency dependence of $\alpha(\nu)/\nu^2$ is expressed by the following form:

$$\frac{\alpha(\nu)}{\nu^2} = \begin{cases} R & (\nu \le \nu_0) \\ r\left(\dfrac{\nu}{\nu_{BP}} + E\right) & (\nu > \nu_0) \end{cases}, \tag{4}$$

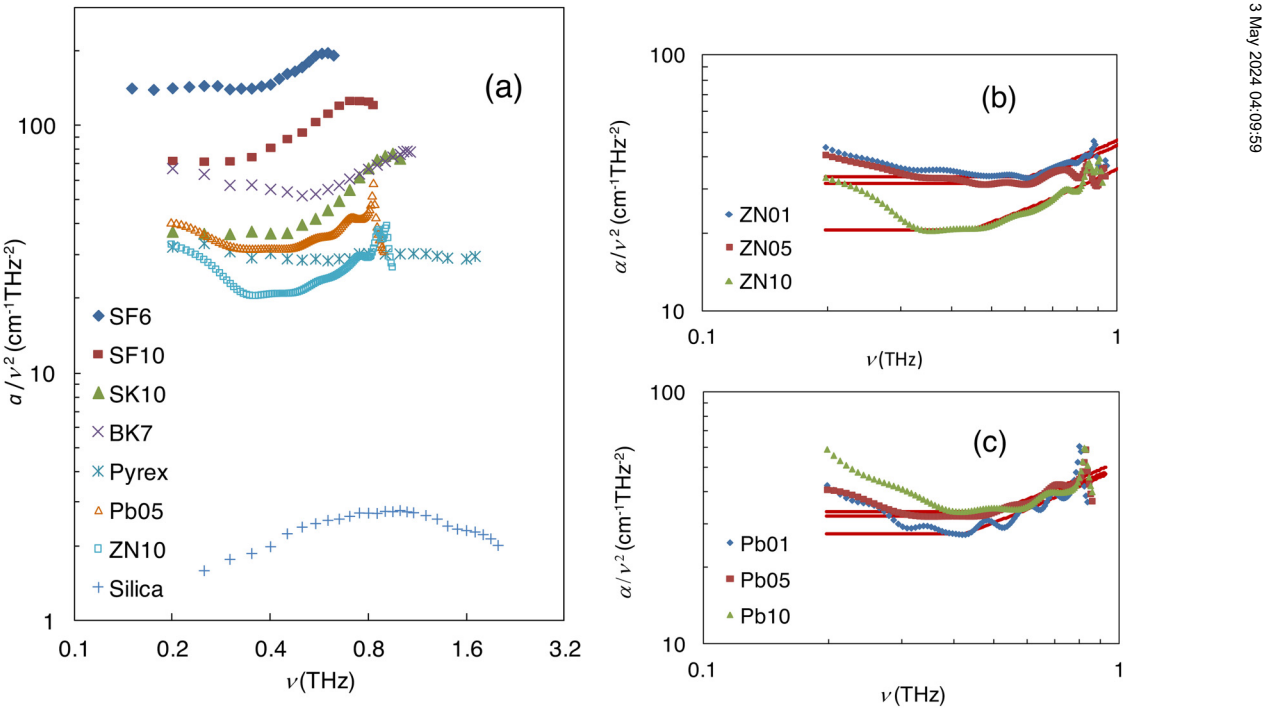

FIG. 3. Plot of α/ν^2 as a function of frequency for (a) various silicate oxide glasses including representative OFS glasses, (b) all ZNbKLSNd glasses, and (c) all PbNKLSNd glasses. Straight lines drawn in (b) and (c) have been obtained by piecewise linear fitting for the varying and minimum (=R) parts of α/ν^2.

TABLE II. Physical parameters determined from the THz-TDS data for a variety of silicate oxide glasses.

Glass	α @0.5THz (cm^{-1})	Kh^2 ($10^{24}\,cm^{-1}s^2$)	β	ν_0 (THz)	ν_{BP} (THz)	R ($cm^{-1}\,THz^{-2}$)	r ($cm^{-1}\,THz^{-2}$)	E E_{av}:0.399
ZNbKLSNd01	8.67	128	1.931	0.617	0.88	33.3	29.1	0.454
ZNbKLSNd 05	8.10	120	2.034	0.612	0.85	31.5	26.6	0.485
ZNbKLSNd 10	5.62	82	2.484	0.474	0.91	20.7	24.5	0.356
PbNKLSNd01	7.57	90	2.162	0.437	0.8	27.3	31.2	0.342
PbNKLSNd05	8.60	104	2.306	0.472	0.83	32.1	32.3	0.434
PbNKLSNd10	8.84	105	2.254	0.552	0.82	33.4	29.0	0.521
Silica	0.62	5.5	2		1	1.6		
Pyrex	7.37	62	1.97		1	28.6		
BK7	17.93	180	2.28	0.571	1.05	52.4	57.5	0.398
SK10	20.62	240	2.8	0.514	0.95	36.7		
SF10	33.49	430	2.38	0.388	0.7	72.2	95.7	0.299
SF6	49.16	700	2.23	0.39	0.58	142	150.5	0.303

where R, r, and E are constants to be determined for each glass material. For fitting the experimental data with Eq. (4), a relation $R = r\,(\nu_0/\nu_{BP} + E)$ should be satisfied because ν_0 is the inflection point frequency. All the parameter values determined from Eq. (4) are included in Table II. As for the value of R for silica, appreciable variation has been observed among different samples (due to, e.g., OH content).[25] In the present analysis, R has been determined to be $1.6\,cm^{-1}THz^{-2}$ by referring to Taraskin's analysis[42] together with Naftaly's analysis ($\alpha = 0.4\,cm^{-1}$ at 0.5 THz)[14] based on Ohsaka's experiment[25] as shown in Table II.

The value of E estimated for different glasses are plotted as a function of Kh^2 in Fig. 5. Although the E value shows a certain variation due to considerably narrow frequency ranges available for the curve fitting as well as data fluctuations, the average value of E is estimated to be 0.4 ± 0.1 for all glasses exhibiting linear frequency dependences. In Fig. 6, the values of R and r determined from Fig. 4 are plotted as functions of Kh^2. High similarity is found between these values, and their proportionality is confirmed in the inset of Fig. 6. This result is consistent with the relation $R = r\,(\nu_0/\nu_{BP} + E)$ because E is constant and ν_0/ν_{BP} does not vary too much for all glasses showing linear behaviors. One may concern with the influence of the sample- or method-dependent differences of ν_{BP} value on the common relation as expressed by Eq. (4). However, it is noticed that there are no distinct dependence between ν_{BP} and the determined parameters such as R, r, or E in the same glass group (e.g., ZNbKLSNd or PbNKLSNd group) within the parameter uncertainty ranges (e.g. < 7% for ν_{BP}). Also, the common feature as expressed by ν/ν_{BP} has been observed over widely different glass groups (ν_{BP} ranging over 0.58–1.05 THz). The observed feature is considered not being influenced by sample- or

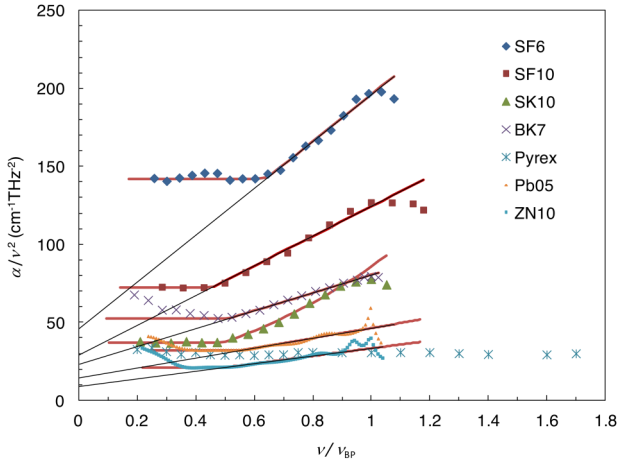

FIG. 4. Relationships of $\alpha(\nu)/\nu^2$ vs normalized frequency ν/ν_{BP} for various silicate oxide glasses. Straight lines indicated linear fittings with varying parts and constant parts of the $\alpha(\nu)/\nu^2$ vs ν/ν_{BP} relations for most of the glasses. A curve obtained by quadratic fitting is shown for SK10 glass data.

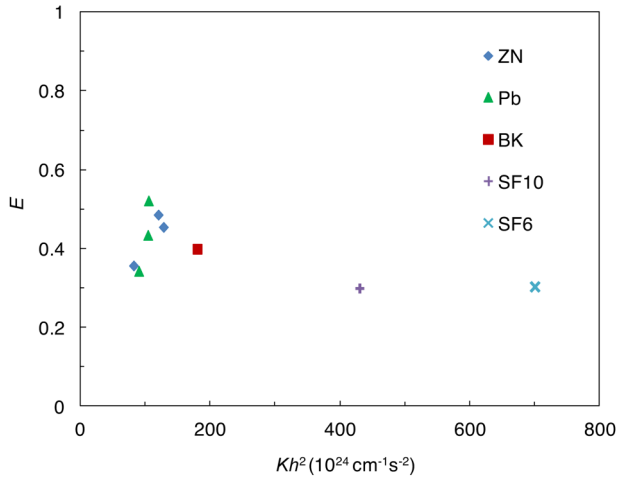

FIG. 5. Plot of values of E as determined in Fig. 4 as a function of absorption parameter Kh^2 for various silicate oxide glasses.

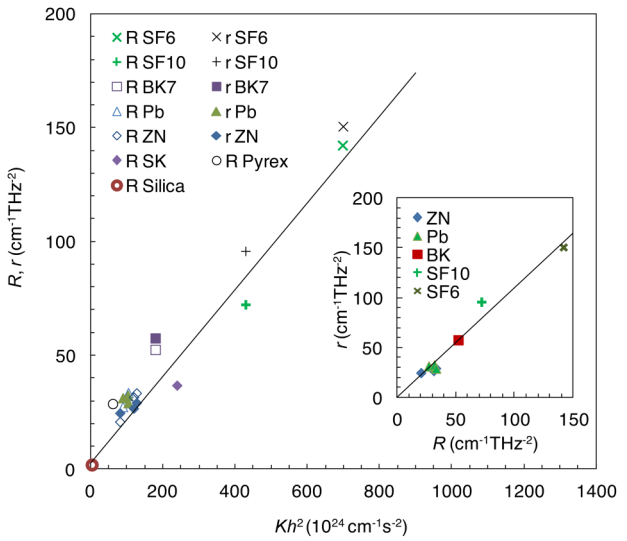

FIG. 6. Plots of R and r as determined in Fig. 4 as a function of absorption parameter Kh^2 for various silicate oxide glasses. Inset shows a relationship between R and r.

method-dependent variations, rather indicating the existence of certain physical/chemical mechanism for the dispersion properties.

C. Discussion on light-vibration coupling coefficient and fluctuating charge

1. vDOS form below boson peak

In order to understand the physical/chemical mechanism of the frequency dependence of $\alpha(\nu)/\nu^2$, we have to consider the effects of both $C_{abs}(\nu)$ and $g(\nu)/\nu^2$ as shown by Eqs. (2) and (3). In particular, the functional form of low frequency edge of vDOS is important to discuss the dispersion property below BP frequency. Since experimental results on vDOS are not available for all the glasses, we have made a survey of published data of $g(\nu)$ spectra for a variety of glassy materials. The $g(\nu)$ spectra collected in this survey have been obtained by neutron inelastic scattering (NIS), heat capacity (HC) experiments, and molecular dynamics (MD) *ab initio* calculations for different silicate oxide glasses covering SiO_2 (NIS[52,53] and MD[42]) and silicate oxides containing alkali ions [$xSiO_2 + (1-x)Y_2O$, Y = Li, Na, and K] (HC[54] and MD[50,55]), $xNb_2O_5 + (1-x)NaPO_3$ glasses (NIS[56]), and protein (lysozyme) material (NIS[49]) for reference. The BP frequency ($\nu_{BP-vDOS}$) was determined from the peak of the reported $g(\nu)/\nu^2$ spectrum. At this frequency, $g(\nu)$ obviously matches the quadratic functional form. The range of the frequency (ν_Q) for which the quadratic function provides a good approximation for $g(\nu)$ has been determined from the reported $g(\nu)/\nu^2$ spectrum [by allowing 5% lowering of $g(\nu)/\nu^2$ from the peak]. These parameters, thus, determined and the ranges of $\nu_Q/\nu_{BP-vDOS}$ are summarized in Table III.

It is noticed in Table III that the quadratic form vDOS is sustained over the $\nu_Q/\nu_{BP-vDOS}$ range from 0.6 to 0.7 to >1.1 and even wider range for a variety of oxide glasses except for silica, for which

TABLE III. Boson peak frequency and quadratic limit frequency ranges determined from vDOS spectra for selected glassy materials.

Material	$g(\nu)\nu^2$ peak frequency $\nu_{BP-vDOS}$ (cm^{-1})	$g\nu \propto \nu^2$ frequency range ν_Q (cm^{-1})	$g(\nu) \propto \nu^2$ frequency range $\nu_Q/\nu_{BP-vDOS}$	Reference
Silica (SiO_2)	24	14–40	0.6–1.7	Richet[54]
Silica (SiO_2)	36	31–40	0.8–1.1	Fabiani[53]
Silica (SiO_2)	30	10–20	0.3–0.7	Taraskin[42]
$2SiO_2 + Li_2O$	80	50–100	0.6–1.3	Richet[54]
$SiO_2 + Na_2O$	35	18–68	0.5–1.9	Richet[54]
$SiO_2 + K_2O$	18	20–60	0.5–2.0	Richet[54]
$Nb_2O_5 + 4NaPO_3$	40	28–50	0.7–1.3	Guo[56]
Lysozyme	20	12–25	0.6–1.2	Mori[49]

definitive vDOS form has not been found in this survey. The obtained $\nu_Q/\nu_{BP-vDOS}$ range seems to be sufficiently wide to cover the linearly ν-dependent $\alpha(\nu)/\nu^2$ behaviors as found in Fig. 4. When assuming such $g(\nu) \propto \nu^2$ form to be applicable to Eq. (3) in the present glass groups, the $\alpha(\nu)/\nu^2$ spectra are considered to provide spectra of the relative value of $C_{abs}(\nu)$. This hypothesis, although it has not been confirmed at this stage in the present particular glasses, is eventually identical, in terms of the frequency dependence, with the Debye model approximation as applied to the low frequency vibrations in various solids.[43] We adopt this assumption in the following discussion to approach plausible mechanism of absorption dispersion in those glasses. The confirmation of exact vDOS form in those glasses is subject to later studies. Concerning the boson peak frequency determination, the $\alpha(\nu)/\nu^2$ peak (ν_{BP}) and $g(\nu)/\nu^2$ peak (ν_{BP-abs}) have been used in Sec. II and in this section, respectively. The ν_{BP} value may become higher than the $\nu_{BP-vDOS}$ value due to the effect of the frequency-dependent term in $C_{abs}(\nu)$. However, this effect can be negligible as far as the frequency dependence is not too steep. In order to focus the general trend of frequency dependence of $C_{abs}(\nu)$, we tentatively use the $\alpha(\nu)/\nu^2$ peak for the BP frequency determination (ν_{BP}) in the following discussion.

2. Relative light-vibration coupling coefficient

Physical interpretation of the observed frequency dependence of $\alpha(\nu)/\nu^2$ is considered in the light of previously reported studies.[42,57] Taraskin *et al.* proposed a universal model of atomic vibrations by using the linear response theory with the harmonic approximation.[42,57] In their theory, the light-vibration coupling coefficient $C_{abs}(\nu)$ is divided into two parts: coherent (giving correlated response) and incoherent (giving uncorrelated response) parts,[58,59] as expressed in the following form:[57]

$$C_{abs}(\nu) = C_{abs}^{incoh}(\nu) + C_{abs}^{coh}(\nu),$$
$$= \frac{2\pi^2 n_{atom}}{c\sqrt{\varepsilon_\infty}} \sum_i \frac{q_i^2}{m_i} \mathbf{e}_i^2(\nu) + \frac{2\pi^2 n_{atom}}{c\sqrt{\varepsilon_\infty}} \sum_{i \neq i'} \frac{q_i q_{i'}}{\sqrt{m_i m_{i'}}} (\mathbf{e}_i(\nu) \cdot \mathbf{e}_{i'}(\nu)), \quad (5)$$

where q_i, m_i, and $\mathbf{e}_i$ (ν) are the fixed but spatially fluctuating atomic charges, mass, and vibrational eigenvector of frequency ν corresponding to atom i (i'), respectively. c stands for the speed of light, ε_∞ represents the high-frequency dielectric constant, and n_{atom} is the atomic number included in the chemical formula. Summations run over atoms (i, i'). In the incoherent term of Eq. (5), all the atoms are regarded as independent absorbing objects, and in contrast, the coherent term takes into account the correlation effects among dipole moments within the summation region where the local charge neutrality is satisfied. It has been shown[42,57] that the incoherent term is independent of the frequency, and this constant value A is correlated with the uncorrelated, fluctuating charge σ_1 by the following equation:

$$A = \frac{2\pi^2\sigma_1^2 n_{atom}}{m_{av}c\sqrt{\varepsilon_\infty}} = \frac{2\pi^2\sigma_1^2\rho}{m_{av}^2 c\sqrt{\varepsilon_\infty}}, \quad (6)$$

where $m_{av} = \rho/n_{atom} = M/n_{atom}/N_A$ is the spatially averaged atomic mass (ρ, density; M, molecular weight; N_A, Avogadro number). Taraskin *et al.* also showed that the coherent term exhibits ν^2-dependence under an assumption of linear dispersion of ν–k characteristics (Debye model) in the low-frequency (FIR) regime. In this case, the coupling coefficient $C_{abs}(\nu)$ is expressed by a form of $C_{abs}(\nu) = A + B\nu^2$ by using material-dependent constants A and B.[42] By taking account of that $g(\nu) \propto \nu^2$ is assumed in the low frequency ($\nu < \nu_{BP}$) range for the present group of glasses, the constant levels R of $\alpha(\nu)/\nu^2$ as observed at low frequencies in all glasses are considered to correspond to the incoherent term of the coupling coefficient (A) and also the ν^2-dependent behavior of $\alpha(\nu)/\nu^2$ as observed for SK10 glass likely represents the coherent term of the coupling coefficient ($B\nu^2$).

In contrast to SK10 glass, other glasses show quite different $\alpha(\nu)/\nu^2$ behavior, exhibiting a constant level R at low frequency followed by shifted linear ν dependence as expressed by Eq. (4) up to the boson peak frequency. Similar light-vibration coupling coefficient behavior has been observed in the absorption in silica glass by Ohsaka[25] and also in Raman scattering in silica glass by Fontana[60] as well as in a variety of materials including oxide and chalcogenide glasses and polymers by Surovtsev.[61] Linear behaviors of the coupling coefficients have been reported recently for both the absorption and Raman scattering below and/or around the boson peak frequency in glucose by Kabeya[48] and in lysozyme by Mori.[49] In lysozyme, the linear coupling coefficient behavior has been observed even above the boson peak frequency, and it has been interpreted by the dispersion relation of the fracton model.[49]

The linear ν-dependences of the absorption coupling coefficient as observed in the present result could appear within Taraskin's model when the linear ν–k dispersion becomes no longer applicable due to, e.g., the damping or dispersion flattening of transverse acoustic mode. The proportionality between R and r as found in Fig. 6 could be understood by speculating that the same dipole oscillator, which is induced by the same ion atom, predominates both the incoherent and coherent contributions of the vibration absorption. As we have shown in our previous work,[39] the low-frequency (sub-THz to THz) oscillators are actually predominated by specific atoms in the glass structure, e.g., Nb in ZNbKLSNd glasses and Na in PbNKLSNd glasses. In Eq. (5), [$\mathbf{e}_i$ (ν) · $\mathbf{e}_{i'}$ (ν)] term gives only a numeral difference between 1 (parallel eigenvectors) and 1/3 (random eigenvectors). If the incoherent/coherent absorption is assumed in a first-order approximation to be governed by the same oscillator, the value of R (uncorrelated contribution, $\propto A$) and r (correlated contribution) would eventually vary in proportion to each other, which gives consistence with the result of $R \propto r$ as found in Fig. 6. The ν^2-dependence of $\alpha(\nu)/\nu^2$ as observed for SK10 glass may be attributable to a different oscillator/bond formation in the glass structure eventually matching with Taraskin's model. The same value of frequency shift ($E \sim 0.4$) as observed for many different glasses implies the existence of a common origin in glass nature, but its detail is subject to further studies.

3. Determination of fluctuating charge in glass structure

On the basis of the discussion made above, the uncorrelated fluctuating charge σ_1 is regarded as a key parameter to control the overall dispersion characteristics of $\alpha(\nu)/\nu^2$, and it is worthwhile knowing their quantities in all glass materials. The value of σ_1 can be estimated by Eq. (6) by using the value reported on SiO_2 as a reference. Using the proportionality between the incoherent coupling coefficient level A and the observed $\alpha(\nu)/\nu^2$ minimum level R in each glass, the value of σ_1 normalized by its SiO_2 value [$\sigma_1/\sigma_1(SiO_2)$] can be determined. By using this ratio and the previously reported values of $\sigma_1 = 0.06e$ (e: electronic charge) for SiO_2,[42] the value of σ_1 has been calculated for each glass, and the results are summarized in Table IV. The relationship between the fluctuating charge σ_1 and the averaged atomic mass m_{av} is shown in Fig. 7.

The silica glass shows the lowest fluctuating charge among all glasses, supporting the lowest fluctuations such as structural disorders and/or chemical bond anomalies introduced in binary oxide materials. Additive atoms with even small contents strongly affect the structural/chemical fluctuation in glass structures, and the absorption loss can be enforced to increase in multi-component

TABLE IV. Result of charge fluctuation parameter characterization for a variety of silicate oxide glasses. The value of ε_∞ determined in Ref. 37 has been used. The value of σ_1 for silica glass has been taken from Ref. 42.

Glass	n_{atom} (/formula)	m_{av} (10^{-23} g)	ε_∞	$\sigma_1/\sigma_1(SiO_2)$	σ_1(e)
ZNbKLSNd01	3.92	5.253	3.28	6.23	0.374
ZNbKLSNd05	4.0	5.521	3.20	6.33	0.380
ZNbKLSNd10	4.1	5.873	3.24	5.57	0.334
PbNKLSNd01	3.07	5.95	2.46	5.90	0.354
PbNKLSNd05	3.15	6.01	2.66	6.53	0.392
PbNKLSNd10	3.25	6.08	2.34	6.68	0.400
Silica	3	3.321	2.13	1	0.06
Pyrex	3.29	3.13	2.16	3.97	0.238
BK7	3.18	3.394	2.31	5.59	0.335
SK10	2.84	6.549	2.62	7.73	0.464
SF10	2.15	11.817	3.00	18.7	1.119
SF6	2.15	13.671	3.28	28.1	1.688

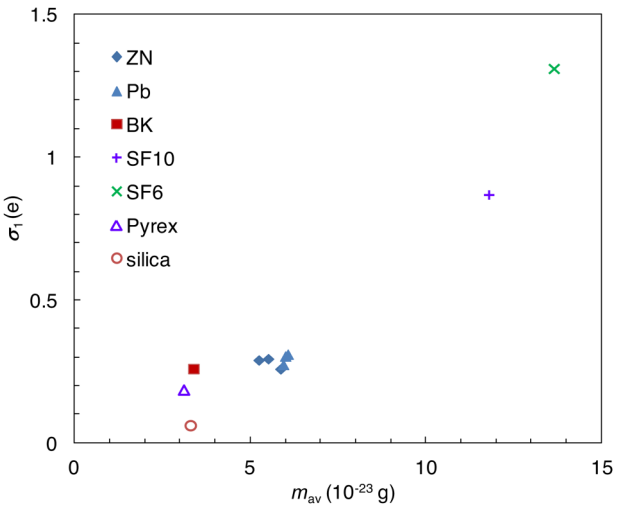

FIG. 7. Plots of fluctuating charges σ_1 in the unit of electronic charge (e) as a function of averaged atomic mass for various silicate oxide glasses.

glasses such as BK7 and Pyrex glasses. OFS glasses exhibit high THz refractive indexes (ZNbKLSNd01: 3.28, and PbNKLSNd05: 2.66, both at 0.5 THz[35]) primarily due to the high polarizability (ZNbKLSNd glasses) and high ionicity (PbNKLSNd glasses).[39] Regardless of appreciable amount of additives introduced in OFS glasses, the absorption minimum levels (R) as well as the fluctuating charges are suppressed to fairly low levels similar to those in BK7 and SK10 glasses. This is attributed to the strain relaxation effects caused by the fluorine addition in OFS glasses.[16,62] On the other hand, very large fluctuating charges are observed in SF series glasses with high contents of heavy metal atoms Pb. This suggests that the Pb-induced contribution to absorption loss is significant and overwhelms the effect of heavy mass [$1/m_{av}^2$ in Eq. (6)]. According to the results described above, the reduction of the structural/chemical fluctuations through the glass composition optimization (e.g., fluorine incorporation and limiting heavy metal content) is effective to reduce both the incoherent (long-range) and coherent (short-range) light-vibration couplings and eventually minimize the sub-THz absorption loss.

IV. CONCLUSION

The frequency dependences of the absorption coefficients in multi-component silicate oxide glasses have been investigated in the frequency region below the boson peak. The normalized frequency (ν/ν_{BP}) dependence of $\alpha(\nu)/\nu^2$ has been found to show a common behavior in most glasses, which exhibits a minimum (constant) level (R) at lower frequency followed by a subsequent linear increase, as is expressed by $\alpha(\nu)/\nu^2 = r\ (\nu/\nu_{BP} + E)$, until the boson peak frequency is reached. It has also been shown that r is proportional to R and E is a common constant (~0.4) for all the glasses exhibiting this behavior. The constant level R is attributed to the uncorrelated charge fluctuation caused by the medium- and long-range structural/chemical fluctuations. The slope r is attributed, under the reasonable vDOS functional form, to the correlated charge fluctuation generated from the short-range disorders maintaining the local charge neutrality in atomic scale. Taking account of the strong link between r and R ($r \propto R$), the absorption dispersion property is controlled primarily by the uncorrelated fluctuating charge (σ_1). σ_1 is, thus, a useful parameter for characterizing the sub-THz absorption dispersion, and its specific value has been determined (from R value) for each glass.

The present study of the sub-THz absorption dispersion in different glasses has led us to the finding of a common dispersion behavior as well as the determination of glass-specific parameters. The obtained results can compensate information missing in the conventional power law-based analysis and will be useful for characterization and design of materials.

ACKNOWLEDGMENTS

The authors acknowledge the Ministry of Science and Technology, Taiwan, for funding support to the present research (Nos. MOST 106-2112-M-007-022-MY2 and MOST 110-2923-E-007-006). Doddoji Ramachari acknowledge the Ministry of Science and Technology, Taiwan, for the award of Postdoctoral Fellowship during this research work. The authors thank Chao-Kai Wang and Chun-Ling Yen for taking the THz-TDS data of the samples reported in this work.

AUTHOR DECLARATIONS

Conflict of Interest

The authors have no conflicts to disclose.

Author Contributions

Osamu Wada: Conceptualization (lead); Data curation (equal); Formal analysis (lead); Investigation (lead); Writing – original draft (lead); Writing – review & editing (equal). **Doddoji Ramachari:** Data curation (equal); Formal analysis (supporting); Methodology (equal); Writing – review & editing (equal). **Chan-Shan Yang:** Data curation (equal); Methodology (equal); Writing – review & editing (equal). **Takashi Uchino:** Investigation (supporting); Writing – review & editing (equal). **Ci-Ling Pan:** Funding acquisition (lead); Resources (lead); Supervision (lead); Writing – review & editing (equal).

DATA AVAILABILITY

The data that support the findings of this study are available from the corresponding author upon reasonable request.

REFERENCES

[1]X:-C Zhang and J.-Z. Xu, *Introduction to THz Wave Photonics* (Springer, 2010), ISBN: 978-1-4419-0977-0.
[2]*Handbook of Terahertz Technology for Imaging, Sensing and Communications*, edited by D. Saeedkia (Woodhead Publishing, 2013), ISBN: 9780857092359, e-ISBN: 9780857096494.
[3]T. Nagatsuma, G. Ducournau, and C. C. Renaud, "Advances in terahertz communications accelerated by photonics," Nat. Photon. **10**(6), 371–379 (2016).
[4]S. Rajabali and I:-C Benea-Chelmus, "Present and future of terahertz integrated photonic devices," APL Photon. **8**, 080901 (2023).

[5]M. S. Islam, C. M. B. Cordeiro, M. J. Nine, J. Sultana, A. L. S. Cruz, A. Dinovitser, B. W.-H. Ng, H. Ebendorff-Heidepriem, D. Losic, and D. Abbott, "Experimental study on glass and polymers: Determining the optimal material for potential use in terahertz technology," IEEE Access **8**, 97204–97214 (2020).
[6]B. You, J.-Y. Lu, C.-P. Yu, T.-A. Liu, and J.-L. Peng, "Terahertz refractive index sensors using dielectric pipe waveguides," Opt. Express **20**(6), 5858–5866 (2012).
[7]M. Zalkovskij, A. C. Strikwerda, K. Iwaszczuk, A. Popescu, D. Savastru, R. Malureanu, A. V. Lavrinenko, and P. U. Jepsen, "Terahertz-induced kerr effect in amorphous chalcogenide glasses," Appl. Phys. Lett. **103**(22), 221102 (2013).
[8]W. Jia, M. Liu, Y. Lu, X. Feng, Q. Wang, X. Zhang, Y. Ni, F. Hu, M. Gong, X. Xu, Y. Huang, W. Zhang, Y. Yang, and J. Han, "Broadband terahertz wave generation from an epsilon-near-zero material," Light Sci. Appl. **10**, 1 (2021).
[9]J.-F. Roux, F. Garet, and J.-L. Coutaz, "Chap. 8, principles and applications of THz time domain spectroscopy," in *Physics and Applications of Terahertz Radiation*, edited by M. Perenzoni and D. J. Paul (Springer, Dordrecht, 2014).
[10]M. Koch, D. M. Mittleman, J. Ornik, and E. Castro-Camus, "Terahertz time-domain spectroscopy," Nat. Rev. Methods Primers **3**, 49 (2023).
[11]S. K. Sundaram, "Chap. 26, terahertz time-domain spectroscopy of glasses," in *Springer Handbook of Glass, Springer Nature*, edited by J. D. Musgraves, J. Hu, and L. Calvez (Gewerbestrasse, Switzerland, 2019).
[12]M. Naftaly and R. E. Miles, "Terahertz time-domain spectroscopy for material characterization," Proc. IEEE **95**(8), 1658–1665 (2007).
[13]O. Wada, D. Ramachari, C–S Yang, T. Uchino, and C–L Pan, "Systematic characterization of high-dielectric constant glass materials using THz-TDS technique," in *Trends in Terahertz Technology*, edited by Y. M. Meziani and J. E. Velázquez-Pérez (IntechOpen, 2023).
[14]M. Naftaly and R. E. Miles, "Terahertz time-domain spectroscopy of silicate glasses and the relationship to material properties," J. Appl. Phys. **102**(4), 043517 (2007).
[15]A. Ravagli, M. Naftaly, C. Craig, E. Weatherby, and D. W. Hewak, "Dielectric and structural characterisation of chalcogenide glasses via terahertz time-domain spectroscopy," Opt. Mater. **69**, 339–343 (2017).
[16]D. Ramachari, C.-S. Yang, O. Wada, T. Uchino, and C.-L. Pan, "High-refractive index, low-loss oxyfluorosilicate glasses for sub-THz and millimeter wave applications," J. Appl. Phys. **125**(15), 151609 (2019).
[17]O. Wada, D. Ramachari, C.-S. Yang, T. Uchino, and C.-L. Pan, "High refractive index properties of oxyfluorosilicate glasses and a unified dielectric model of silicate oxide glasses in sub-terahertz frequency region," Opt. Mater. Express **10**(2), 607–621 (2020).
[18]A. Pacewicz, J. Cimek, B. Salki, M. Walczakowski, and R. Buczynski, "Reconstruction and modeling of the complex refractive index of nonlinear glasses from terahertz to optical frequencies," Opt. Express **29**(16), 26191 (2021).
[19]N. J. Tostanoski and S. K. Sundaram, "Universal power-law of terahertz optical properties of borosilicate, tellurite, and chalcogenide glass families," Sci. Rep. **13**, 2260 (2023).
[20]M. F. Ando, O. Benzine, Z. Pan, J:-L Garden, K. Wondraczek, S. Grimm, K. Schuster, and L. Wondraczek, "Boson peak, heterogeneity and intermediate-range order in binary SiO_2-Al_2O_3 glasses," Sci. Rep. **8**, 5394 (2018).
[21]D. K. Dobesh, S. K. Sundaram, and R. E. Youngman, "'Femtosecond laser pulse-induced structural modification of lanthanum aluminosilicate glasses: Refractive indices in visible vs.: Terahertz frequency regions," J. Infrared Millimeter Terahertz Waves **41**, 171–193 (2020).
[22]U. Strom, J. R. Hendrickson, R. I. Wagner, and P. C. Taylor, "Disorder-induced far infrared absorption in amorphous materials," Solid State Commun. **15**(11/12), 1871–1875 (1974).
[23]U. Strom and P. C. Taylor, "Temperature and frequency dependences of the far-infrared and microwave optical absorption in amorphous materials," Phys. Rev. B **16**(12), 5512–5522 (1977).
[24]T. Nakayama, "Boson peak and terahertz frequency dynamics of vitreous silica," Rep. Prog. Phys. **65**(8), 1195–1242 (2002).
[25]T. Ohsaka and S. Oshikawa, "Effect of OH content on the far-infrared absorption and low-energy states in silica glass," Phys. Rev. B **57**(9), 4995–4998 (1998).
[26]W. Schirmacher, G. Ruocco, and T. Scopigno, "Acoustic attenuation in glasses and its relation with the boson peak," Phys. Rev. Lett. **98**, 025501 (2007).
[27]S. Gelin, H. Tanaka, and A. Lemaître, "Anomalous phonon scattering and elastic correlations in amorphous solids," Nat. Mater. **15**, 1177–1181 (2016).
[28]U. Buchenau, Y. M. Galperin, V. L. Gurevich, and H. R. Schober, "Anharmonic potentials and vibrational localization in glasses," Phys. Rev. B **43**, 5039–5045 (1991).
[29]V. L. Gurevich, D. A. Parshin, and H. R. Schober, "Anharmonicity, vibrational instability, and the boson peak in glasses," Phys. Rev. B **67**, 094203 (2003).
[30]S. N. Taraskin, Y. L. Loh, G. Natarajan, and S. R. Elliott, "Origin of the boson peak in systems with lattice disorder," Phys. Rev. Lett. **86**, 1255–1258 (2001).
[31]A. I. Chumakov, G. Monaco, A. Monaco, W. A. Crichton, A. Bosak, R. Rüffer, A. Meyer, F. Kargl, L. Comez, D. Fioretto, H. Giefers, S. Roitsch, G. Wortmann, M. H. Manghnani, A. Hushur, Q. Williams, J. Balogh, K. Parliński, P. Jochym, and P. Piekarz, "Equivalence of the boson peak in glasses to the transverse acoustic van Hove singularity in crystals," Phys. Rev. Lett. **106**, 225501 (2011).
[32]W. Steurer, A. Apfolter, M. Koch, W. E. Ernst, B. Holst, E. Søndergård, and J. R. Manson, "Observation of the boson peak at the surface of vitreous silica," Phys. Rev. Lett. **99**, 035503 (2007).
[33]J.-L. Tao, Z.-Y. Yang, and Y.-J. Wang, "Structural rationale for boson peak in metallic glass informed by an interpretable neural network model," Phys. Rev. Res. **5**, 023113 (2023).
[34]M. González-Jiménez, T. Barnard, B. A. Russell, N. V. Tukachev, U. Javornik, L.-A. Hayes, A. J. Farrell, S. Guinane, H. M. Senn, A. J. Smith, M. Wilding, G. Mali, M. Nakano, Y. Miyazaki, P. McMillan, G. C. Sosso, and K. Wynne, "Understanding the emergence of the boson peak in molecular glasses," Nat. Commun. **14**, 215 (2023).
[35]M. Naftaly and A. Gregory, "Terahertz and microwave optical properties of single-crystal quartz and vitreous silica and the behavior of the boson peak," Appl. Sci. **11**, 6733 (2021).
[36]S. Tsuzuki, N. Kuzuu, H. Horikoshi, K. Saito, K. Yamamoto, and M. Tani, "Influence of OH-group concentration on optical properties of silica glass in terahertz frequency region," Appl. Phys. Express **8**, 072402 (2015).
[37]O. Wada, D. Ramachari, C.-S. Yang, T. Uchino, and C.-L. Pan, "Systematic characterization of THz dielectric properties of multi-component glasses using unified oscillator model," Opt. Mater. Express **11**(3), 858–874 (2021).
[38]O. Wada, D. Ramachari, C.-S. Yang, and C.-L. Pan, "Interrelationship among dielectric constant, energy band parameters and ionicity in multi-component oxide glasses revealed by optical- and THz-band spectroscopy," J. Non-Crystall. Solids **573**, 121135 (2021).
[39]O. Wada, D. Ramachari, C.-S. Yang, Y. Harada, T. Uchino, and C.-L. Pan, "Mechanism of THz dielectric constant enhancement in multi-component oxide glasses investigated by infrared and THz spectroscopies," J. Phys. Chem. Solids **176**, 111237 (2023).
[40]C.-S. Yang, M.-H. Lin, C.-H. Chang, P. Yu, J.-M. Shieh, C.-H. Shen, O. Wada, and C.-L. Pan, "Non-drude behavior in indium-tin-oxide nanowhiskers and thin films investigated by transmission and reflection THz time-domain spectroscopy," IEEE J. Quant. Electron. **49**(8), 677–690 (2013).
[41]F. L. Galeener, A. J. Leadbetter, and M. W. Stringfellow, "Comparison of the neutron, Raman, and infrared vibrational spectra of vitreous SiO_2, GeO_2, and BeF_2," Phys. Rev. B **27**(2), 1052–1078 (1983).
[42]S. N. Taraskin, S. I. Simdyankin, S. R. Elliott, J. R. Neilson, and T. Lo, "Universal features of terahertz absorption in disordered materials," Phys. Rev. Lett. **97**, 055504 (2006).
[43]H. Ibach and H. Lüth, "Chap. 5," in *Solid-State Physics: An Introduction to Principles of Materials Science*, 2nd ed. (Springer-Verlag, Berlin, 1996).
[44]A. I. Chumakov, I. Sergueev, U. van Bürck, W. Schirmacher, T. Asthalter, R. Rüffer, O. Leupold, and W. Petry, "Collective nature of the boson peak and universal transboson dynamics of glasses," Phys. Rev. Lett. **92**(24), 245508 (2004).
[45]M. Naftaly and R. E. Miles, "Terahertz time-domain spectroscopy: A new tool for the study of glasses in the far infrared," J. Non-Crystall. Solids **351**, 3341–3346 (2005).

[46]R. Szal, J. Zmojda, M. Kochanowicz, P. Miluski, J. Dorosz, M. Lesniak, P. Jeleń, B. Starzyk, M. Sitarz, M. Kuwik, J. Pisarska, W. A. Pisarski, Y. Iijima, T. Mori, and D. Dorosz, "Spectroscopic properties of antimony modified germanate glass doped with Eu^{3+} ions," Ceram. Int. **45**, 24811–24817 (2019).
[47]J. Kölbel, W. Schirmacher, E. Shalaev, and J. A. Zeitler, "Terahertz dynamics in the glycerol-water system," Phys. Rev. B **107**, 104203 (2023).
[48]M. Kabeya, T. Mori, Y. Fujii, A. Koreeda, B. W. Lee, J.-H. Ko, and S. Kojima, "Boson peak dynamics of glassy glucose studied by integrated terahertz-band spectroscopy," Phys. Rev. B **94**, 224204 (2016).
[49]T. Mori, Y. Jiang, Y. Fujii, S. Kitani, H. Mizuno, A. Koreeda, L. Motoji, H. Tokoro, A. Shiraki, Y. Yamamoto, and S. Kojima, "Detection of boson peak and fractal dynamics of disordered systems using terahertz spectroscopy," Phys. Rev. E **102**, 022502 (2020).
[50]E. P. J. Parrott, J. A. Zeitler, G. Simon, B. Hehlen, L. F. Gladden, S. N. Taraskin, and S. R. Elliott, "Atomic charge distribution in sodosilicate glasses from terahertz time-domain spectroscopy," Phys. Rev. B **82**, 140203(R) (2010).
[51]J. J. Bian, H. Wang, and H. J. Wang, "THz dielectric properties of $AlPO_4$-BPO_4-SiO_2 ternaries," J. Eur. Ceram. Soc. **43**, 5530–5534 (2023).
[52]A. J. Dianoux, "Neutron scattering by low-energy excitations of disordered materials," Philos. Mag. B **59**(1), 17–31 (1989).
[53]E. Fabiani, A. Fontana, and U. Buchenau, "Neutron scattering study of the vibrations in vitreous silica and germania," J. Chem. Phys. **128**, 244507 (2008).
[54]N. F. Richet, "Heat capacity and low-frequency vibrational density of states: Inferences for the boson peak of silica and alkali silicate glasses," Physica B **404**, 3799–3806 (2009).
[55]S. Ispas, N. Zotov, S. De Wispelaere, and W. Kob, "Vibrational properties of a sodium tetrasilicate glass: *Ab initio* versus classical force fields," J. Non-Crystall. Solids **351**, 1144–1150 (2005).
[56]Y. Guo, "Raman spectroscopy of glasses with high and broad Raman gain in the boson peak region," Ph.D. thesis (University of Central Florida, 2006), Electronic theses and dissertations, 2004–2019. 996, see https://stars.library.ucf.edu/etd/996
[57]S. N. Taraskin, S. I. Simdyankin, and S. R. Elliott, "The atomic charge distribution in glasses obtained by terahertz spectroscopy," J. Phys.: Cond. Matter **19**(45), 455216 (2007).
[58]S. W. Lovesey, *Theory of Neutron Scattering From Condensed Matter, Vol. 1: Nuclear Scattering* (Clarendon Press, Oxford, 1984), ISBN: 9780198520283.
[59]B. Rufflé, M. Foret, and B. Hehlen, "Chap. 7, Low-frequency vibrational spectroscopy of glasses," in *Low-Temperature Thermal and Vibrational Properties of Disordered Solids: A Half-Century of Universal "Anomalies" of Glasses*, edited by M. A. Ramos (World Scientific, 2022), pp. 227–298, ISBN: 978-1-80061-259-4 (e-book).
[60]A. Fontana, R. Dell'Anna, M. Montagna, F. Rossi, G. Viliani, G. Ruocco, M. Sampoli, U. Buchenau, and A. Wischnewski, "The Raman coupling function in amorphous silica and the nature of the long-wavelength excitations in disordered systems," Europhys. Lett. **47**(1), 56–62 (1999).
[61]N. V. Surovtsev and A. P. Sokolov, "Frequency behavior of Raman coupling coefficient in glasses," Phys. Rev. B **66**, 054205 (2002).
[62]H. Hosono, M. Mizuguchi, L. Skuja, and T. Ogawa, "Fluorine-doped SiO_2 glasses for F_2 excimer laser optics: Fluorine content and color-center formation," Opt. Lett. **24**(22), 1549–1551 (1999).